

Polymer Translocation Induced by a Bad Solvent

Christopher Lörcher,¹ Tapio Ala-Nissila,^{2,3} and Aniket Bhattacharya^{1,*}

¹*Department of Physics, University of Central Florida,
Orlando, Florida 32816-2385, USA*

²*Department of Applied Physics, Aalto University School of Science and Technology,
P.O. Box 11000, FI-00076 Aalto, Espoo, Finland*

³*Department of Physics, Box 1843, Brown University,
Providence, Rhode Island 02912-1843, USA*

(Dated: June 9, 2010)

Abstract

We employ 3D Langevin Dynamics simulations to study the dynamics of polymer chains translocating through a nanopore in presence of asymmetric solvent conditions. Initially a large fraction ($> 50\%$) of the chain is placed at the *cis* side in a good solvent while the *trans* segments are placed in a bad solvent that causes the chain to collapse and promotes translocation from the *cis* to the *trans* side. In particular, we study the ratcheting effect of a globule formed at the *trans* side created by the translocated segment, and how this ratchet drives the system towards faster translocation. Unlike in the case of unbiased or externally forced translocation where the mean first passage time $\langle\tau\rangle$ is often characterized by algebraic scaling as a function of the chain length N with a single scaling exponent α , and the histogram of the mean first passage time $P(\tau/\langle\tau\rangle)$ exhibits scaling, we find that scaling is not well obeyed. For relatively long chains we find $\langle\tau\rangle \sim N^\alpha$ where $\alpha \approx 1$ for $\varepsilon/k_B T > 1$. In this limit, we also find that translocation proceeds with a nearly constant velocity of the individual beads(monomers), which is attributed to the coiling of the globule. We provide an approximate theory assuming rotational motion restricted on a 2D disc to demonstrate that there is a crossover from diffusive behavior of the center of mass for short chains to a single file translocation for long chains, where the average translocation time scales linearly with the chain length N .

PACS numbers: 87.15.A-, 87.15.H-, 36.20.-r

*Author to whom the correspondence should be addressed; Electronic address: aniket@physics.ucf.edu

I. INTRODUCTION

Attempts to understand the dynamics of viral invasion and infection [1], dynamics of DNA and other biopolymers passing through porous media (*i.e.* cell membranes), and direct medical applications such as gene therapy and drug delivery, have rendered the field of polymer translocation a very active field of research in recent years [2, 3]. Much work has been done to understand the physics involved in the translocation process. Analytical work by Sung and Park [4], Muthukumar [6], Chuang, Kantor and Kardar [7, 8], Dubbeldam and coworkers[9], Panja and coworkers[10], and others[11–13], supplemented by a vast amount of numerical work [14]–[21], has brought profound physical insight into the problem at hand. In particular, much has been learned about making translocation faster in a controllable fashion, as this should be beneficial in biological systems.

To this end, a process known as Brownian ratcheting [22] was discovered early on and discussed further in Refs.[23]–[27]. Brownian ratchets are mechanisms by which translocation can be driven, or carried out more efficiently[27]. As discussed by Simon, Peskin, and Oster[22], thermal or chemical asymmetries in the system can be used to extract useful work (*i.e.* translocation of the polymer) from the thermal bath in accordance with the Second Law of Thermodynamics [27]. As the polymer translocates, it experiences considerable back and forth motion due to thermal fluctuations. If the part of the chain that is on the *trans* side is modified in such a way as to prevent backward motion through the pore, its random motion will be biased and translocation through the pore is notably faster [24]. This modification to the chain which causes a biased translocation is often called a Brownian ratchet [22]. A Brownian ratchet can manifest itself in many different ways. There can exist binding particles that bind as chaperones on the *trans* side [25, 28], glycosylation can be used [24], or the chain can be tightly bound into a coil on the *trans* side via some method, usually by having a bad solvent [16] or reducing the solvent’s pH [24]. In a bad solvent, the polymer chain undergoes a coil-globule transition to form a highly interacting spherical-like polymeric configuration with a radius of gyration R_g that scales with the number of monomers N as $\langle R_g \rangle \sim N^{1/3}$ [29, 30].

In the present work, our aim is to study the influence of ratcheting on the dynamics of polymer translocation as induced by an asymmetry in solvent quality between the *cis* and *trans* compartments. We focus on the case of two-sided translocation [14], where a fraction

of the polymer chain is initially placed at the *trans* compartment, with good solvent on the *cis* side and bad solvent on the *trans* side. This asymmetry in the solvent condition induces a bias in the entropic barrier controlling translocation in such a way as to effectively drive the polymer to the *trans* side. To characterize the dynamics of translocation, we analyze the waiting times, velocities, and effective forces on the individual monomers inside the pore. We find that for long chains with high attraction strengths, $\varepsilon/k_B T$, waiting times vary only slightly until the last beads emerge, at which point entropic effects become dominant. Since the velocity of the beads is inversely proportional to the waiting time, we get roughly constant velocity in this regime. This is apparent only for long chains with relatively high interaction strengths; for shorter chains with lower interaction strengths, the center of mass velocity of the polymer introduces an N dependence into the velocity that cannot be overlooked when calculating how the average translocation time scales with N . We used this idea to make an approximate estimate for the N dependence of the average translocation time. We find for short chains the translocation exponent $\alpha \approx 2$, while in the large N limit, we find $\alpha \rightarrow 1$. We end our analysis by analyzing the histograms of the mean first passage time(MFPT). We note that since α varies between 2 and 1, we do not see universal scaling for a given value of $\varepsilon/k_B T$. However, in the large N limit, we begin to see scaling manifest itself clearly, with a scaling exponent approaching the predicted value of unity.

II. MODEL

We use the Langevin equation to study the Brownian motion of particles in solution. It is a statistical, stochastic differential equation of the form for each bead i :

$$m\ddot{\mathbf{r}}_i(t) = -\nabla U_i - \Gamma \dot{\mathbf{r}}_i(t) + \mathbf{W}_i(t), \quad (1)$$

where the total interaction,

$$U_i = U_{FENE}^i + \sum U_{LJ}^{ij}, \quad (2)$$

is the sum of the finitely extensible nonlinear elastic(FENE) spring potential interaction [31]

$$U_{FENE}(r_{ij}) = -\frac{1}{2}kR_0^2 \ln \left[1 - \left(\frac{r_{ij}}{R_0} \right)^2 \right], \quad (3)$$

and the Lennard-Jones interaction between neighboring monomers,

$$U_{LJ}(r_{ij}) = 4\varepsilon_{ij} \left[\left(\frac{\sigma_{ij}}{r_{ij}} \right)^{12} - \left(\frac{\sigma_{ij}}{r_{ij}} \right)^6 - \left(\frac{\sigma_{ij}}{r_{ij}^c} \right)^{12} + \left(\frac{\sigma_{ij}}{r_{ij}^c} \right)^6 \right]. \quad (4)$$

The term $\mathbf{W}(t)$ describes the influence of Markovian white noise due to the solvent, which is not taken into account explicitly here. It satisfies the fluctuation-dissipation relation

$$\langle \mathbf{W}(t) \cdot \mathbf{W}(\tau) \rangle = 6k_B T \Gamma \delta_{ij} \delta(t - \tau). \quad (5)$$

To model asymmetric solvent conditions on the *cis* and *trans* sides, interaction cut-off values were modified using a cut-off matrix. Each particle was given a label (either 1 or 2, depending on whether it was on the *cis* side or *trans* side, respectively). The cutoff values for the *trans* side were set higher ($r_{c,22} = 2.5\sigma$) than those for the *cis* side ($r_{c,11} = r_{c,12} = r_{c,21} = 2^{1/6}\sigma$). This ensures that the monomers on the *trans* side interact with a “bad” solvent[32], while the monomers on the *cis* side are in a good solvent characterized by a self avoiding random walk with Flory exponent $\nu = 0.588$ ($R_g \sim N^\nu$) in 3D. The different cut-off values introduce a chemical potential difference, $\Delta\mu$, between the compartments. We will study the corresponding solvent asymmetry for various monomer-monomer interaction coupling strengths, ε . In particular, we will study how this solvent quality asymmetry drives the system towards a much faster translocation.

The purely repulsive wall consists of one monolayer of immobile LJ particles of diameter 1.5σ on a *triangular lattice* at the *xy* plane at $z = 0$. The pore is created by removing the particle at the center. The reduced units of length, time and temperature are chosen to be σ , $\sigma\sqrt{\frac{m}{\varepsilon}}$, and ε/k_B respectively. For the spring potential we have chosen $k = 30$ and $R_{ij} = 1.5\sigma$, the friction coefficient $\Gamma = 1.0$, and the temperature is kept at $1.5/k_B$ throughout the simulation.

For a chosen fraction of the monomers at the *cis/trans* we equilibrate the chain for a time on the order of the Rouse relaxation time $\tau \sim N^{1+2\nu}$, where the Flory exponent $\nu = 0.588$ in 3D. The chain is then allowed to translocate using a time step of $dt = 0.005$. As the last bead exits the pore, a translocation event is completed and the process repeated for 2000 times for averaging.

One way to understand the dynamics of a polymer chain translocating under such highly asymmetric conditions, is to study the analytic form of its free energy. Following Muthukumar, the free energy for m translocated monomers is given by [5]

$$\frac{\mathcal{F}_m}{k_B T} = (1 - \gamma'_2) \ln(m) + (1 - \gamma'_1) \ln(N - m) + m \frac{\Delta\mu}{k_B T}. \quad (6)$$

Here, $\gamma' = 0.5, 0.69$, and 1 for Gaussian, self-avoiding, and rod-like chains, respectively. Driving force is easily obtained from the free energy by differentiating with respect to monomer

index:

$$\frac{1}{k_B T} \frac{\partial \mathcal{F}_m}{\partial m} = (1 - \gamma'_2) \frac{1}{m} + (1 - \gamma'_1) \frac{1}{(m - N)} + \frac{\Delta\mu}{k_B T}. \quad (7)$$

This is the driving force of the system in units of $k_B T$ for particular values of γ'_1 , γ'_2 , and $\Delta\mu$. As we shall demonstrate below, there is a delicate balance between the frictional and driving forces that will tend to set the system at a constant velocity.

The translocation time for a chain is a function of the number of monomers on the *trans* side at the beginning of the translocation process $N_{tr}(t = 0)$. If we start our simulation having 50% of the chain on the *trans* side, corresponding to the “two-sided” translocation first considered in Ref. [14], *i.e.* $N_{tr}(t = 0)/N = 0.5$, this corresponds to releasing the chain down a downhill entropic barrier and therefore, the probability for successful translocation, $P(N_{tr}(t = 0))$, should be unity, which is indeed the case in our simulation. This probability decreases drastically as the fraction $N_{tr}(t = 0)/N$ is less than 0.5, and especially for long chains, the probability for a successful translocation is very small as shown in Fig. 1 for a chain of length $N = 64$. In the present work, we have studied the cases for $N_{tr}(t = 0) = 0.5N$ and $N_{tr}(t = 0) = 0.25N$. By comparing these two sets of data, we have extracted the results for the limit $N_{tr}(t = 0) \rightarrow 0$. As expected, we recover uniform scaling of the probability distribution for the MFPT with a translocation scaling exponent $\alpha \rightarrow 1$ in the large N limit.

III. RESULTS AND DISCUSSION

To get an idea of the translocation process, we show typical snapshots of a translocating chain in Fig. 2(a) and Fig. 2(b) at different stages of the translocation process. At $t = 0$, the fraction of the chain that is located on the *cis* side is characterized by the equilibrium Flory exponent $\nu \simeq 0.588$, that corresponds to the good solvent condition. Since the *trans* part of the chain is in a poor solvent and the temperature is below the Θ -temperature [32], it will form a globule which is expected to grow as a function of time. Comparing the snapshots for $\varepsilon/k_B T = 0.5$ (Fig. 2(a)) and $\varepsilon/k_B T = 1.5$ (Fig. 2(b)), we note that the globule formed by the translocated segments becomes more compact as the strength of the interaction increases. We have checked the N dependence of the radius of gyration for chains immediately after the translocation process as shown in Fig. 3. For larger interaction strength, we find $R_g \sim N^{0.37}$, which is consistent with the N dependence of a compact spherical globule. It is worth mentioning that if all the globules for different chain lengths

were perfect spheres and fully relaxed, then $R_g \sim N^{0.33}$. For $\varepsilon/k_B T = 1.5$, we note from the snapshots that the spheres are very compact and hence a dependence of $R_g \sim N^{0.37}$ implies that the spheres formed by the translocated segments for different chain lengths are close to equilibrium. For $\varepsilon/k_B T = 0.5$, the corresponding exponent extracted from the slope of $N = 64, 128$ and 256 yields $R_g \sim N^{0.26}$, which is less than $1/3$. This indicates that the *trans* side of the chain does not have sufficient time to relax during the translocation process as discussed earlier in the literature[11, 18, 19, 21].

We have monitored several quantities during the translocation process. First, we have analyzed the waiting time as a function of monomer index (Fig. 4), where we have defined waiting time to be the total time each bead spends at the pore divided by the total translocation time $\langle \tau \rangle$ for the whole chain to cross the pore (*i.e.* $W(m) = \langle \tau(m) \rangle / \langle \tau \rangle$), where $\tau(m)$ is the total time bead m spends at the pore). The notation $\langle \cdot \rangle$ indicates ensemble average over 2000 iterations. We notice that $W(m)$ initially increases and then decreases to almost zero, and the position of the maximum increases with the chain length N . We also find that the peak position is an increasing function of the interaction strength $\varepsilon/k_B T$. Previously, waiting time of a monomer for a translocating chain was studied in great detail[14]. For a homopolymer undergoing externally forced translocation, the residence time increases and becomes maximum for a monomer index $m_{max} > N/2$; it then decreases (more rapidly than the rise) almost linearly, the position of the maximum being skewed towards $m > N/2$. When an attractive interaction is present for the translocated segments, the barrier that the monomers at the *cis* side are pulled through is effectively skewed. However, this is different from applying a force only on the monomer inside the pore. We note that data in Fig. 4 are similar to the case of forced translocation. However, for the last $\sim 10\%$ of monomers, the residence time decreases very rapidly. This becomes more pronounced with increasing strength of the attractive interaction. It is evident from the residence time plots that longer chains with larger attraction strengths result in residence times that vary only slightly over the trajectory of the translocation, until the last beads emerge. We note that the waiting time of each monomer is inversely proportional to the velocity of that particular monomer at the pore. We have plotted the reciprocal of the waiting time function (scaled by the appropriate factors) for a chain length of $N = 128$ (Fig. 5). We note that the velocity and inverse waiting time function collapse onto the same graph and are relatively constant up to the last few beads, at which point they both drastically increase due to entropic forces.

We will explore the velocity at the pore for all the chains lengths below.

The behavior of the residence time when translated to the average velocity of the monomer at the pore for various chain lengths $N = 16 - 256$ and for $\varepsilon/k_B T = 0.5, 1.0$ and 1.5 is shown in Figs. 6 (a)-(c). As predicted from the residence time plots, the velocity for long chains is virtually constant for the entire translocation process until the end, when the last beads emerge from the pore. We note that the driving force should be proportional to the velocity. From Eqn. (7) given for the driving force, we note that the term involving the reciprocal of the difference $N - m$, blows up as the last few beads emerge from the pore, explaining why velocity increases for the last few beads at the pore. This is most evident for longer chains with higher $\varepsilon/k_B T$ (Fig. 6(b)-(c)).

To further understand our results, we have studied the force experienced at the pore as a function of the monomer index Fig. 7(a)-(c). In order to get a better idea about the interaction of the chain with different solvents on either side of the pore we have not shown the force arising out of the high frequency phonons from the anharmonic spring potential and have shown only the LJ contribution to the force in our plots. For $\varepsilon/k_B T = 0.5 - 1.5$ and relatively long chains, we see a rather flat force curve, which is close to $F = 0$, in agreement with $v = \text{const}$ discussed earlier (Fig. 7(a)). We interpret this result as being indicative of a force balance between frictional and driving forces F_f and F_{dr} , respectively, at the pore. The driving force F_{dr} is given by $\frac{\partial \mathcal{F}_m}{\partial m}$ in Eqn. (7.) For force balance to occur, we must then have the following condition:

$$\langle F_{dr} \rangle \approx \langle F_f \rangle. \quad (8)$$

In the large N limit, the driving force will be governed primarily by the chemical potential difference between the compartments $\Delta\mu$. In this limit

$$\langle F_{dr}(N \rightarrow \infty) \rangle \approx \Delta\mu \approx \Gamma \langle V(N \rightarrow \infty) \rangle. \quad (9)$$

Thus, we see that the coiling velocity v_c will be proportional to the chemical potential difference:

$$\langle v_c \rangle \approx \frac{\Delta\mu}{\Gamma} \approx \text{const}. \quad (10)$$

The main result is that in the large N limit, the driving force and velocity are independent of N and only dependent on the chemical potential difference between the compartments. This driving force is exactly balanced by the friction experienced by the monomers, which is

proportional to the velocity of the beads. Thus we see that in the large N limit the condition $\sum F \approx 0$ and $v \approx \text{const}$ is well obeyed.

In the case of short chains, the force becomes negative gradually for the last beads, whereas for long chains the change is rather drastic (Fig. 7(a)-(c)). We interpret this negative force as being a result of the last few beads, (having a relatively large velocity) while still being at the *cis* compartment but in the vicinity of the pore, getting absorbed by the globule on the *trans* compartment, resulting in a deceleration as they escape the *cis* compartment. This results in a negative force on the last few monomers.

Next we present a simple scaling argument for estimating how the average translocation time should scale as a function of N . It is based on the observation that the translocation dynamics corresponds to a “coiling” of the chain around the collapsed globule on the *trans* side with coiling velocity v_c (Fig. 8). If we assume that the attractive force F_e on the bad solvent side is directed towards the center of the globule, we can write $F_e \sim mv_c^2/R$, which gives $v_c \sim (RF_e/m)^{1/2}$. For the collapsed globule close to equilibrium $R \sim N^{1/3}$ and $m \sim N$, and thus $v_c \sim (N^{-2/3}F_e)^{1/2}$. Due to spherical symmetry, we expect that the force will be proportional to the number of monomers in a disk of radius $R \sim N^{1/3}$. Thus, $F_e \sim N^{2/3}$, from which we extract that $v_c = \text{const}$. Now, $\langle \tau \rangle v \sim R_g^3$, where $R_g^3 \sim N$ and $v = 1/N + v_c = 1/N + \text{const}$. The $1/N$ dependence comes from the velocity of the center of mass, and will only contribute in the low N limit. Thus we can see that in the low N limit, the $1/N$ term dominates and thus $\langle \tau \rangle \sim N^2$, which is supported by our results below. On the other hand, for large N , the constant will dominate, thus arriving at the large N limit of $\langle \tau \rangle \sim N$, also supported below. Thus for single file translocation induced by coiling, we would expect a scaling exponent close to $\alpha \approx 1$, much lower than 3D forced translocation where $\alpha \approx 1.37 - 1.6$ depending on the rate of translocation [17, 18, 20, 21].

We have tested the scaling argument above for several values of ε by studying the histograms of the MFPT for several values of chain length, namely $N = 16, 32, 64, 128$, and 256 to see how they scale as a function of N . Following previous work[20] we have used nonlinear regressions of the form $f(x) = Ax^B \exp(-Cx)$. The maxima for these curves occur at $x = B/C$. We have used the position of the maxima for each chain length to obtain the mean first passage time $\langle \tau \rangle$ from which we can extract the scaling exponents given in Table I. Scaled MFPT histograms are shown in Fig. 9(a)-(c) for $\varepsilon/k_bT = 0.5 - 1.5$. We notice from Table I that the scaling exponent α decreases when extracted from successive larger values

of N . If we look at the spectrum of exponents calculated for short and long chains and for various values of the interaction strength ε qualitatively we notice that for short chains and weaker ε the exponent reflects diffusive behavior, while for larger combination of N and ε the exponent is less than the corresponding exponent for forced translocation for similar chain lengths [17, 18, 20, 21]. In the next section we provide theoretical argument why the translocation behavior from short N and low ε is dominated by diffusive behavior while for long N and large ε , this diffusive behavior crosses over to a “single file” translocation asymptotically reaching a scaling exponent $\alpha \rightarrow 1$ in this limit. Evidently, for this reason we do not see data collapse of the scaled histogram for the MFPT accros the board. However, it is worth noticing that for long N and large ε ($N = 128$ and 256 and $\varepsilon/k_B T = 1.5$) we notice a near perfect data collapse. One can see this trend from Eqn. (7). For short chains we see that chain length plays quite an important role in determining the driving force on the polymer. For relatively long chains, as we showed earlier, this N dependence is washed away, and the only contribution to the driving force is the chemical potential difference. Thus for $N \rightarrow \infty$ the driving force becomes independent of chain length.

We have also compared how the MFPT data collapse on a single master curve when we use the initial condition, $N_t(t = 0) = N/4$ instead of $N_t(t = 0) = N/2$ as shown in Fig. 10. We notice that data collapse and scaling is more closely obeyed in this regime. The scaling exponent for $\varepsilon/k_B T = 1.5$ continues to suggest a tendency towards $\alpha \rightarrow 1.0$ in the large N limit, as is also predicted by Wei *et al.* in their studies of the effect of solvent quality asymmetries on the translocation process [16], although studied differently and using a different model for the solvent conditions. Their studies indicate that polymers translocating under different solvent qualities have a scaling law that varies from $\langle \tau \rangle \sim N^{1+2\nu}$ to $\langle \tau \rangle \sim N$, which is quite close to our results. Our present results are also consistent with Muthukumar’s analytical expression for the translocation time as a function of N for various conditions for the chemical potential difference [5]. Calculations in Muthukumar’s work show that for symmetric barriers, the translocation time will scale as $\langle \tau \rangle \sim N^2$. For asymmetric barriers and long chains, if the entropic terms in the free energy equation are small compared to the term involving $\Delta\mu$, then the translocation time scales linearly as $\langle \tau \rangle \sim N$ for $N\|\Delta\mu\| > 1$, and scales as $\langle \tau \rangle \sim N^2$ for $N\|\Delta\mu\| < 1$, which is consistent with our present results. For relatively short chains (*i.e.* $N = 16$) and weak coupling strength ε , we note a scaling exponent close to $\alpha \approx 2$. For longer chains with stronger coupling

constants ε , we notice a trend towards unity, in complete agreement with Muthukumar's analytic expression. We expect that for longer chains, this limit will be even more closely reached due to the single file nature of the translocation induced by the coiling of the globule on the bad solvent compartment. This is also reflected in in Fig. 11(a)-(c) we show the translocation time $\langle\tau\rangle$ plotted against N on a log-log scale. In each attempt to scale the MFPT histograms, we have used the linear fit slope of the entire log-log plot (*i.e* $\langle\tau\rangle \sim N^\alpha$). The exponents support our claim that the the translocation interpolates from diffusive to a single file behavior.

IV. SUMMARY AND CONCLUSIONS

We have investigated using 3D Langevin Dynamics simulations the properties of a homopolymer translocating through a nano-pore with a solvent asymmetry. In our model, there is good solvent on the *cis* side of the pore, while on the *trans* side there is bad solvent. This creates an effective driving force on the polymer and leads to the emergence of a collapsed globule on the *trans* side during the translocation process. We have used a free energy argument to show that the driving force is relatively insensitive to chain length in the large N limit and is governed mainly by the chemical potential difference between the compartments. As is evident from our force plots, there is a delicate balance between this constant (in the large N limit) driving force and the friction force experienced by the beads. Consistent with this idea, we find that the velocity of the beads at the pore is relatively constant in the large N limit, which is attributed the constant coiling velocity occurring on the "trans" compartment. Furthermore, we note that scaling is not well obeyed in the low N limit as is evident from our mean first passage time histograms. We interpret this as being a consequence of the N dependence of the driving force (and thus velocity!) in the low N limit. For longer chains, however, we note that the driving force(and velocity) become quite insensitive to changes in the chain length, and we retrieve scaling with a scaling law close to our predicted large N limit of $\langle\tau\rangle \sim N$. This can be interpreted as a crossover phenomenon from diffusive type translocation to a single-file driven translocation. Our studies might be relevant for translocation of biopolymers accros cell membranes.

V. ACKNOWLEDGEMENTS:

CJL at the University of Central Florida has been supported by the Florida Education Fund (McKnight Doctoral Fellowship). AB acknowledges funds from Department of Applied Physics, Aalto University School of Science and Technology for a visiting Professorship during summer 2009. TAN acknowledges travel fund from University of Central Florida during May 2009 and funds by the Academy of Finland through the COMP CoE and TransPoly consortium grants.

REFERENCES:

-
- [1] B. Alberts *et al.*, *Molecular Biology of the Cell* (Garland Publishing, New York, 1994).
 - [2] A. Meller, J. Phys.:Condens. Matter.**15**, R581 (2003).
 - [3] M. Muthukumar, Annu. Rev. Biophys. Biomol. Struc **36**, 435 (2007).
 - [4] W. Sung and P. J. Park, Phys. Rev. Lett. **77**, 783 (1996); P. J. Park and W. Sung, J. Chem. Phys. **108**, 3013 (1998).
 - [5] M. Muthukumar, *J. Chem. Phys.* **111**, 10371 (1999).
 - [6] M. Muthukumar, Phys. Rev. Lett. **86**, 3188 (2000).
 - [7] J. Chuang, Y. Kantor, and M. Kardar, Phys. Rev. E **65**, 011802 (2001).
 - [8] Y. Kantor and M. Kardar, Phys. Rev. E **69**, 021806 (2004).
 - [9] J. L. A. Dubbeldam, A. Milchev, V. G. Rostiashvili, and T. A. Vilgis, Phys. Rev. E **76**, 010801(R) (2007); J. L. A. Dubbeldam, A. Milchev, V. G. Rostiashvili, and T. A. Vilgis, Europhys. Lett. **79**, 18002 (2007).
 - [10] D. Panja, G. T. Barkema, and R. C. Ball, J. Phys.: Condens. Matter **19**, 432202 (2007); *ibid*, **20**, 075101 (2008); J. K. Wolterink, G. T. Barkema, and D. Panja, Phys. Rev. Lett. **96**, 208301 (2006); H. Vocks, D. Panja, G. T. Barkema, and R. C. Ball, J. Phys.: Condens. Matter **20**, 095224 (2008).
 - [11] T. Sakaue, Phys. Rev. E **76**, 021803 (2007); *ibid* **81**, 041808 (2010).
 - [12] M. G. Gauthier and G. W. Slater, J. Chem. Phys. **128**, 065103 (2008); *ibid*, **128**, 205103 (2008).
 - [13] A. Milchev, K. Binder, and A. Bhattacharya, J. Chem. Phys. **121**, 6042 (2004).
 - [14] K. Luo, T. Ala-Nissila, and S.C. Ying, *J. Chem. Phys.* **124**, 034714 (2006); K. Luo, I. Huopaniemi, T. Ala-Nissila, and S.-C. Ying, J. Chem. Phys. **124**, 114704 (2006); K. Luo, T. Ala-Nissila, S.-C. Ying, and A. Bhattacharya, J. Chem. Phys. **126**, 145101 (2007).
 - [15] K.F. Luo, T. Ala-Nissila, S.C. Ying, and A. Bhattacharya, *Phys. Rev. Lett.* **99**, 148102 (2007); *ibid*, *Phys. Rev. Lett.* **100**, 058101 (2008).
 - [16] D. Wei, W. Yang, X. Jin, and Q. Liao, J. Chem. Phys. **126**, 204901 (2007).
 - [17] K. Luo, Santtu T. T. Ollila, I. Huopaniemi, T. Ala-Nissila, P. Pomorski, M. Karttunen, S.-C.

- Ying, and A. Bhattacharya, Phys. Rev. E **78**, 050901(R) (2008).
- [18] K. Luo, T. Ala-Nissila, S.-C. Ying and R. Metzler, Europhys. Lett. **88**, 68006 (2009).
 - [19] V. V. Lehtola, R. P. Linna, and K. Kaski, Europhys. Lett. **85**, 58006 (2009); Phys. Rev. E **78**, 061803 (2008).
 - [20] A. Bhattacharya, W. Morrison, K. Luo, T. Ala-Nissila, S.-C. Ying, A. Milchev, and K. Binder, Eur. Phys. J. E **29**, 423 (2009).
 - [21] A. Bhattacharya and K. Binder, Phys. Rev. E **81**, 041804 (2010).
 - [22] S. Simon, C. Peskin, and G. Oster, Proc. Natl. Acad. Sci U.S.A. **89**, 3770 (1992).
 - [23] C. Peskin, G.M. Odell, and G. Oster, Biophys. J. **65**, 316 (1993).
 - [24] P. De Gennes, Proc. Natl. Acad. Sci U. S. A. **96**, 7262 (1996).
 - [25] R. Zandi, D. Reguera, J. Rudnick, and G.M. Gelbart, Proc. Natl. Acad. Sci U. S. A. **100** 8649 (2003).
 - [26] H. Salaman, D. Zbaida, Y. Rabin, D. Chatenay, Proc. Natl. Acad. Sci U. S. A **98**, 7247 (2001).
 - [27] *For a nice pedagogical treatment of Brownian ratchet see* R. P. Feynman, *The Feynman Lectures on Physics, Vol. 1.* (Addison-Wesley, Massachusetts, 1963).
 - [28] A. Bhattacharya, C. J. Lorsch, T. Ala-Nissila, and W. Sung, *Bulletin of the American Physical Society*, APS March Meeting 2010 **55**, Session B10 and unpublished.
 - [29] P. J. Flory, *Principles of Polymer Chemistry.* (Cornell University Press, Ithaca, 1953)
 - [30] I. Nishio, S.-T. Sun, G. Swislow, and T. Tanaka, Nature **281**, 208 (1979).
 - [31] G.S. Grest, K. Kremer, Phys. Rev. A **33** 3628 (1986).
 - [32] The Θ -temperature for the parameters used in this work has already been determined. For example please see H. Liu, A. Bhattacharya, and A. Chakrabarti, J. Chem. Phys. **111** 11183 (1999).

FIGURE CAPTIONS

Fig. 1: Probability of successful translocation as a function of the initial number of monomers on the *trans* side for a chain of length $N = 64$.

Fig. 2(a): Snapshots of a translocating chain of length $N = 256$ for $\varepsilon/k_B T = 0.5$ at times (a) $t = 0$, (b) 0.25τ , (c) 0.5τ , (d) 0.75τ , and (e) 1.0τ respectively.

Fig. 2(b): Snapshots of a translocating chain of length $N = 256$ for $\varepsilon/k_B T = 1.5$ at times (a) $t = 0$, (b) 0.25τ , (c) 0.5τ , (d) 0.75τ , and (e) 1.0τ respectively.

Fig. 3: Variation of $\langle R_g \rangle$ as a function of number of translocated monomer N_{tr} (log-log plot) for $\varepsilon/k_B T = 1.5$ (black circles) and $\varepsilon/k_B T = 0.5$ (red squares) respectively.

Fig. 4: Average waiting time as a function of monomer index normalized by the maximum waiting time for various chain lengths. The symbols circles (black), squares (red), diamonds (green), triangle up (blue), and triangle left (magenta) correspond to the chain lengths $N = 16, 32, 64, 128$, and 256 respectively (color online) for (a) $\varepsilon/k_B T = 0.5$. (b) $\varepsilon/k_B T = 1.0$, and (c) $\varepsilon/k_B T = 1.5$.

Fig. 5: Inverse of waiting time (red diamonds) and velocity of the monomer beads (blue circles) plotted as a function of monomer index for chain length $N = 128$ and $\varepsilon/k_B T = 0.5$. We note that the two graphs almost fall on top of each other and are relatively constant until the end of the translocation, when the last beads emerge out of the pore.

Fig. 6: Average velocity on the monomer beads inside the pore as a function of monomer index for chain lengths $N = 16, 32, 64, 128$, and 256 respectively for (a) $\varepsilon/k_B T = 0.5$, (b) $\varepsilon/k_B T = 1.0$, and (c) $\varepsilon/k_B T = 1.5$. The symbols have the same meaning as in Fig. 4. We note that in the large N limit, the velocity of the monomers becomes almost constant excepting for the last few monomers.

Fig. 7: Average force on the monomer beads inside the pore as a function of monomer index for chain lengths $N = 16, 32, 64, 128$, and 256 respectively for (a) $\varepsilon/k_B T = 0.5$, (b)

$\varepsilon/k_B T = 1.0$, and (c) $\varepsilon/k_B T = 1.5$. The symbols have the same meaning as in Fig. 4. To analyze the force, we have taken only the LJ contribution (neglected the smallest the fluctuations). In agreement with the velocity plots, we notice that the force at the pore is not only constant, but also zero in the large N limit, which agrees with the constant velocity that we find at the pore, indicating a force balance at the pore between friction and driving force. We also notice that the force drastically becomes negative as the last few beads translocates.

Fig. 8: Schematic of a polymer coiling ideally around a collapsed globule. The force is directed towards the center and is proportional the number of monomers in a 2D disc around which the translocating polymer coil.

Fig. 9: Scaled histograms for the MFPT for different chain lengths $N=16, 32, 64, 128$, and 256 for (a) $\varepsilon/k_B T = 0.5$, (b) $\varepsilon/k_B T = 1.0$, and (c) $\varepsilon/k_B T = 1.5$ for $N_{tr}(t=0)/N = 0.5$. The symbols have the same meaning as in Fig. 4. Here, we have used the linear fit slope for the entire Log-Log plots (Fig. 11) for $\varepsilon/k_B T = 0.5 - 1.5$ as scaling exponents. In general for these values of $\varepsilon/k_B T$ we do not notice universal scaling for all chain length N . However, for longer chains and larger attraction strengths (inset in (b) and (c)), we begin to see scaling emerges quite clearly for $\alpha \approx 1$.

Fig. 10: (a) Unscaled and scaled MFPT Histograms for chain length $N = 64$ (green diamonds) and $N = 128$ (blue triangle-ups) with $N_{tr}/N(t=0) = 0.25$ as the initial condition. (a) for $\varepsilon/k_B T = 0.5$ where we notice a scaling exponent close to the value attained for the corresponding case of $N_{tr}/N(t=0) = 0.50$ shown in Fig. 9. (b) For $\varepsilon/k_B T = 1.5$; we notice a scaling exponent closer to the theorized large N limit of unity. We also note that scaling is more closely obeyed in this case.

Fig. 11: Variation of $\langle \tau \rangle$ as a function of N (log-log plot) for (a) $\varepsilon/k_B T = 0.5$, (b) $\varepsilon/k_B T = 1.0$, and (c) $\varepsilon/k_B T = 1.5$ respectively. The local values of the slope (α) are indicated in the graph.

Table I: Effective scaling exponents ($\langle\tau\rangle \sim N^\alpha$) for various combinations of N and $\frac{\varepsilon}{k_B T}$

N	$\frac{\varepsilon}{k_B T} = 0.5$	$\frac{\varepsilon}{k_B T} = 1.0$	$\frac{\varepsilon}{k_B T} = 1.5$
16-32	2.0	1.5	1.3
32-64	1.6	1.10	1.1
64-128	1.3	1.10	1.2
128-256	1.2	1.1	1.2

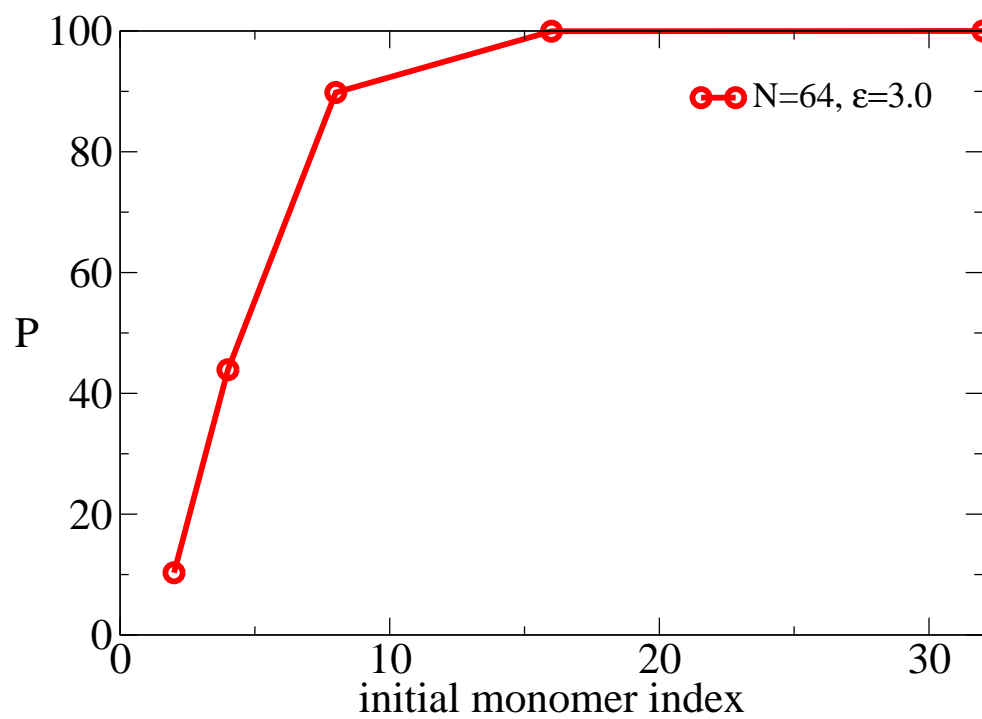


Fig. 1

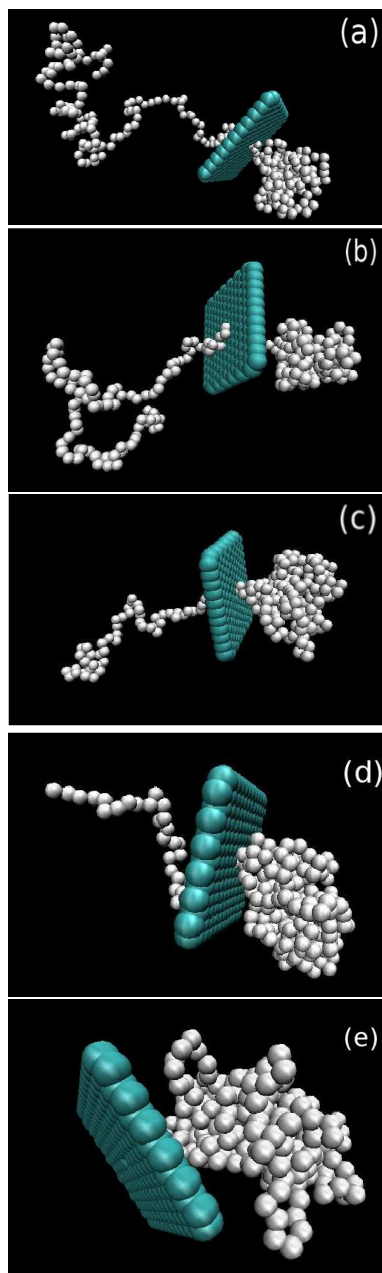


Fig. 2(a)

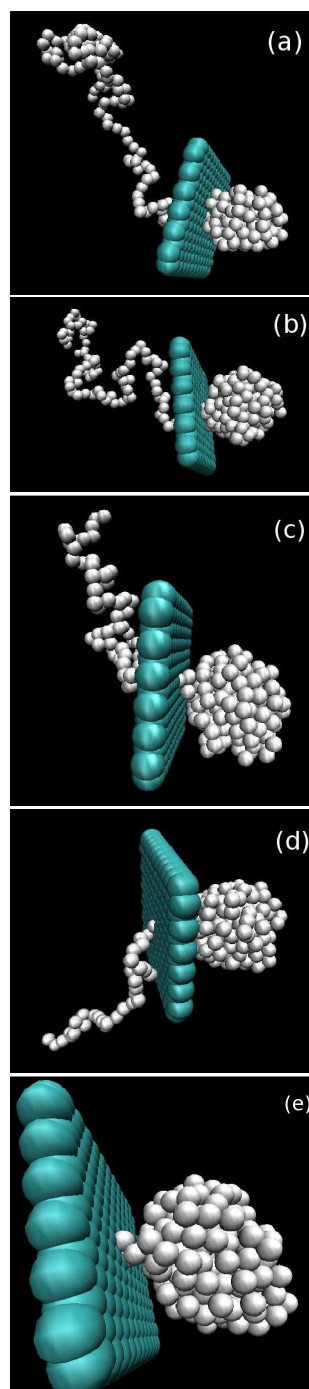


Fig. 2(b)

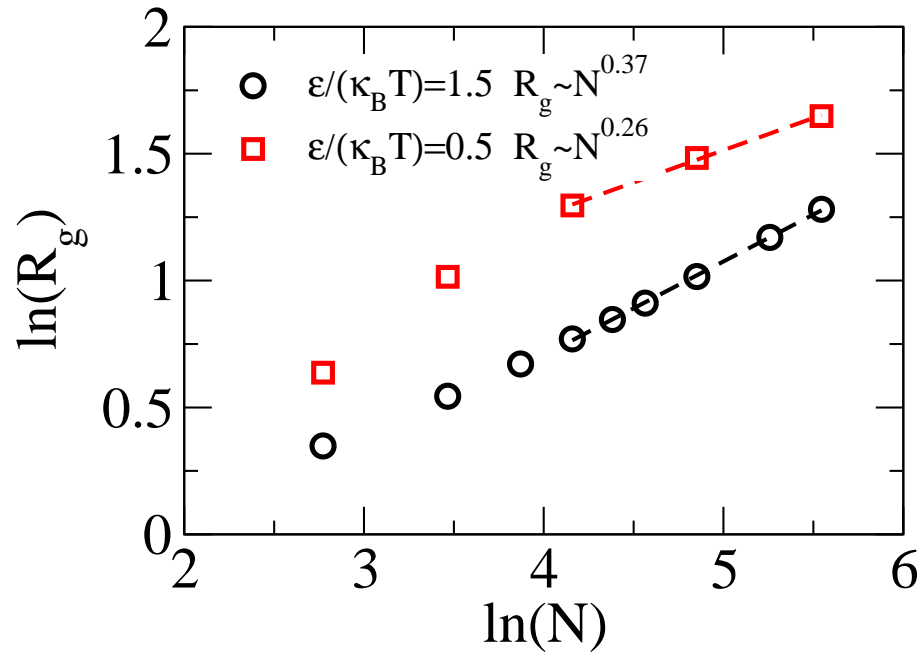


Fig. 3

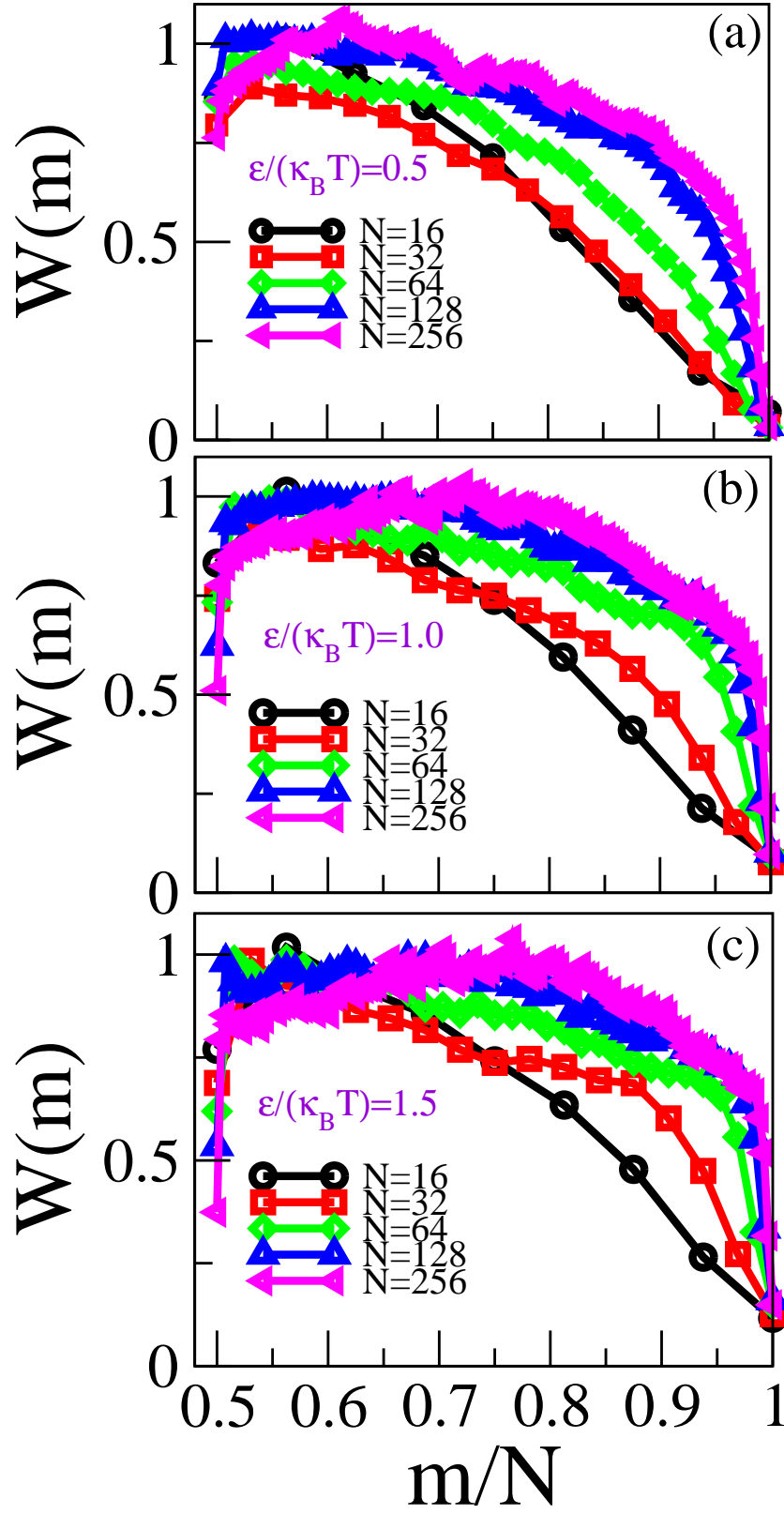


Fig. 4

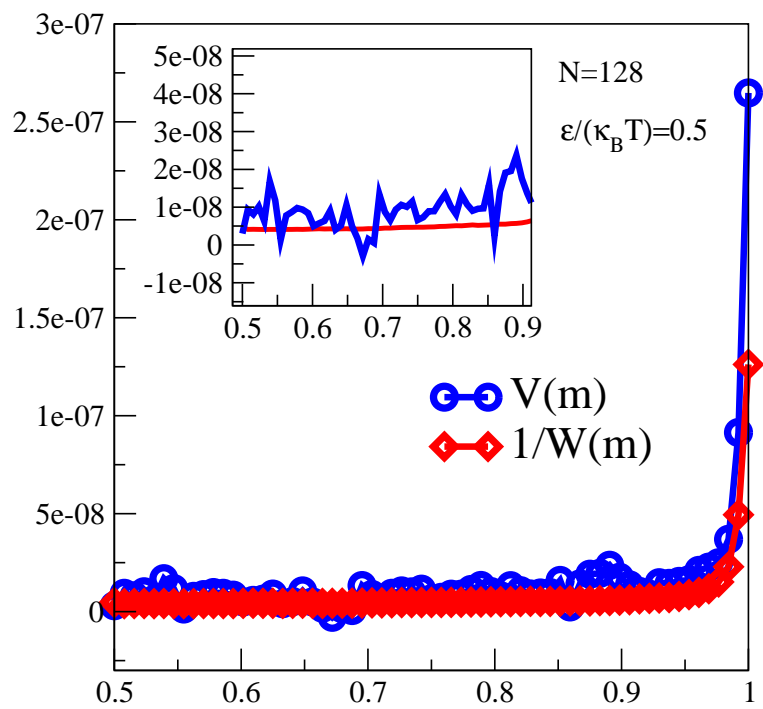


Fig. 5

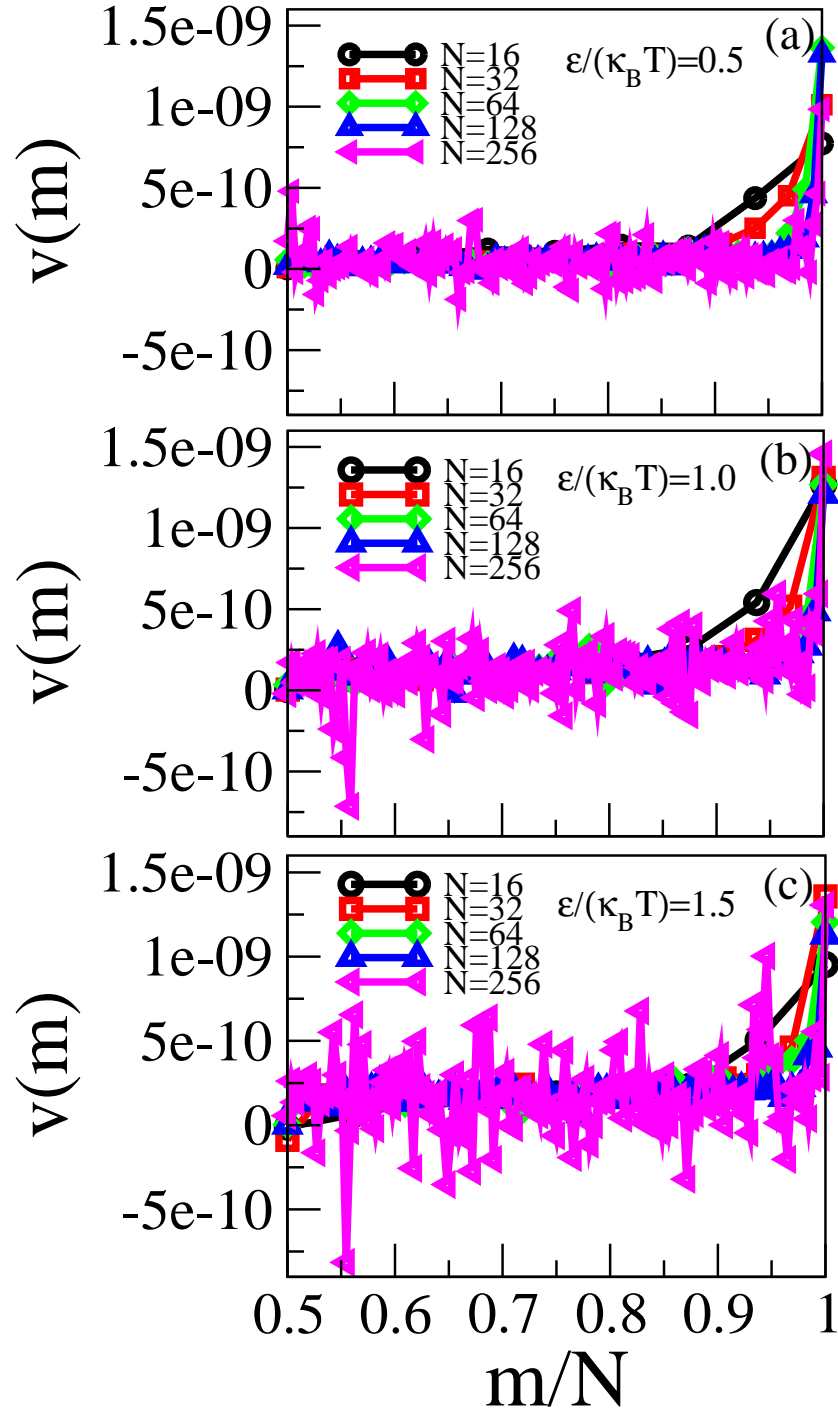


Fig. 6

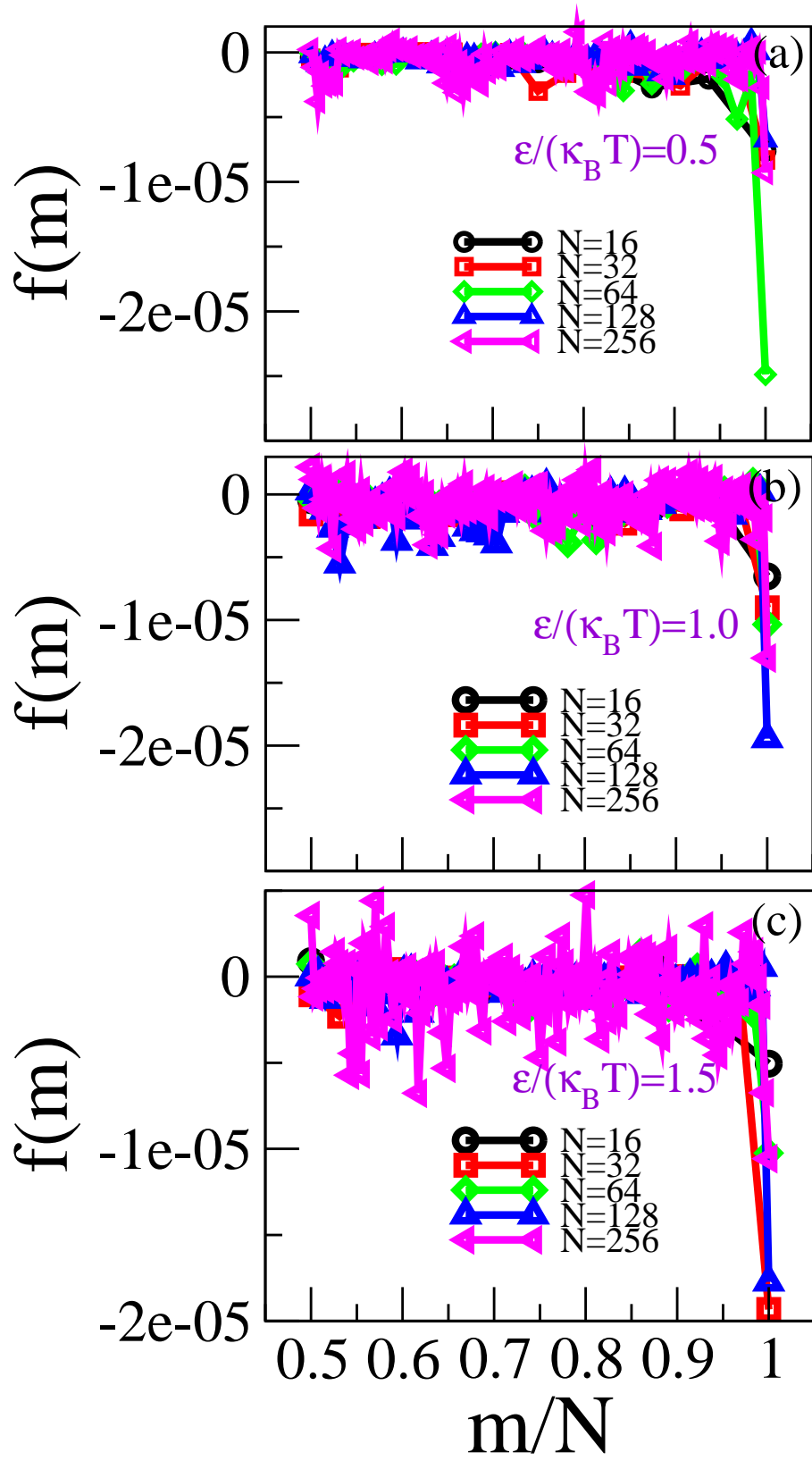


Fig. 7

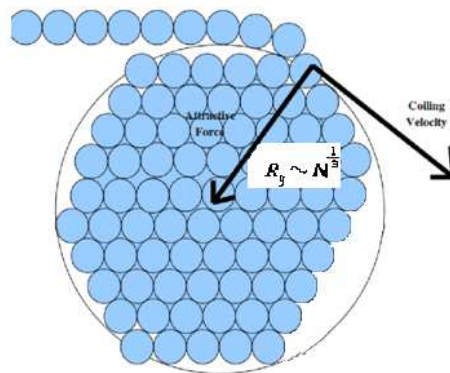


Fig. 8

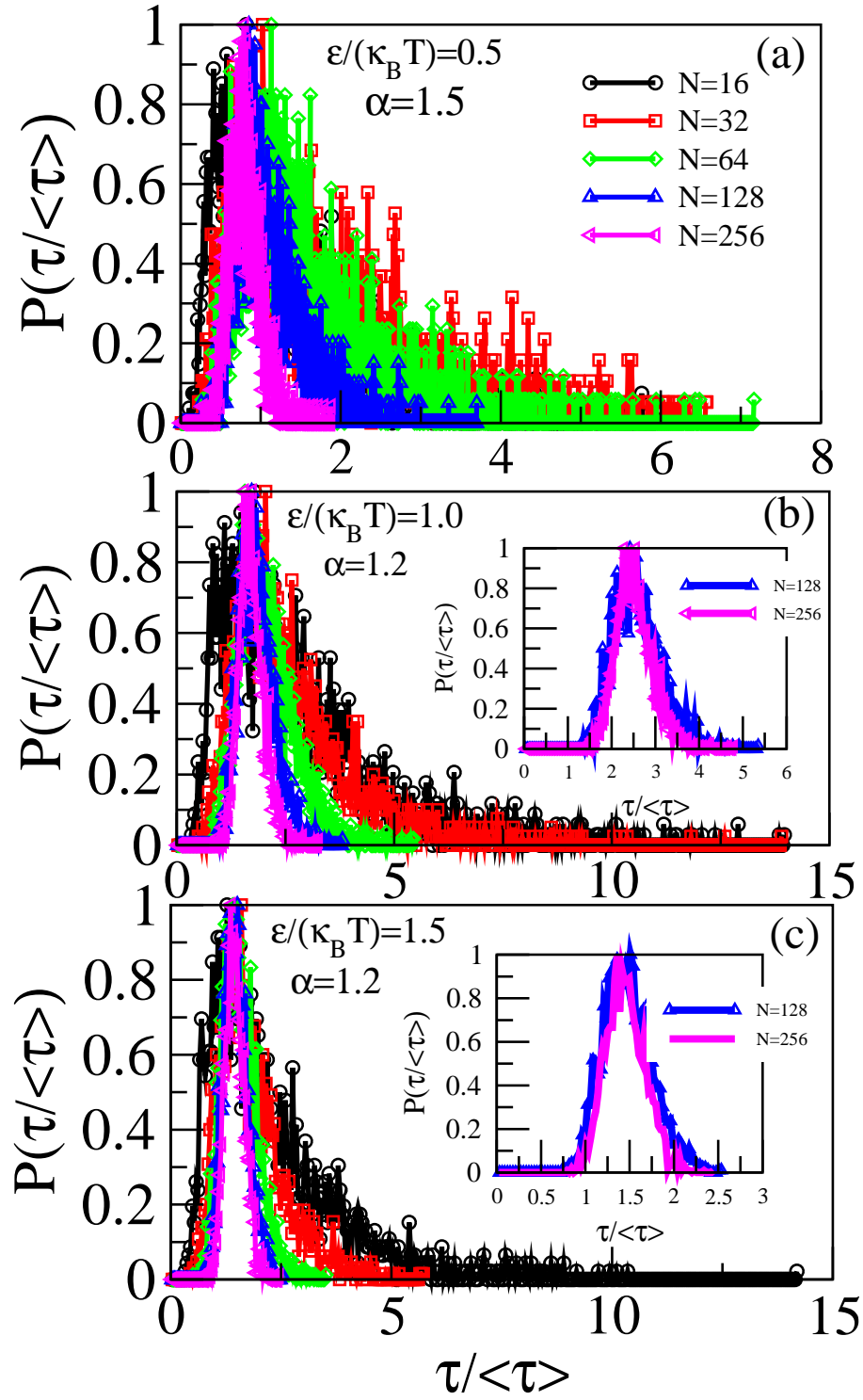


Fig. 9

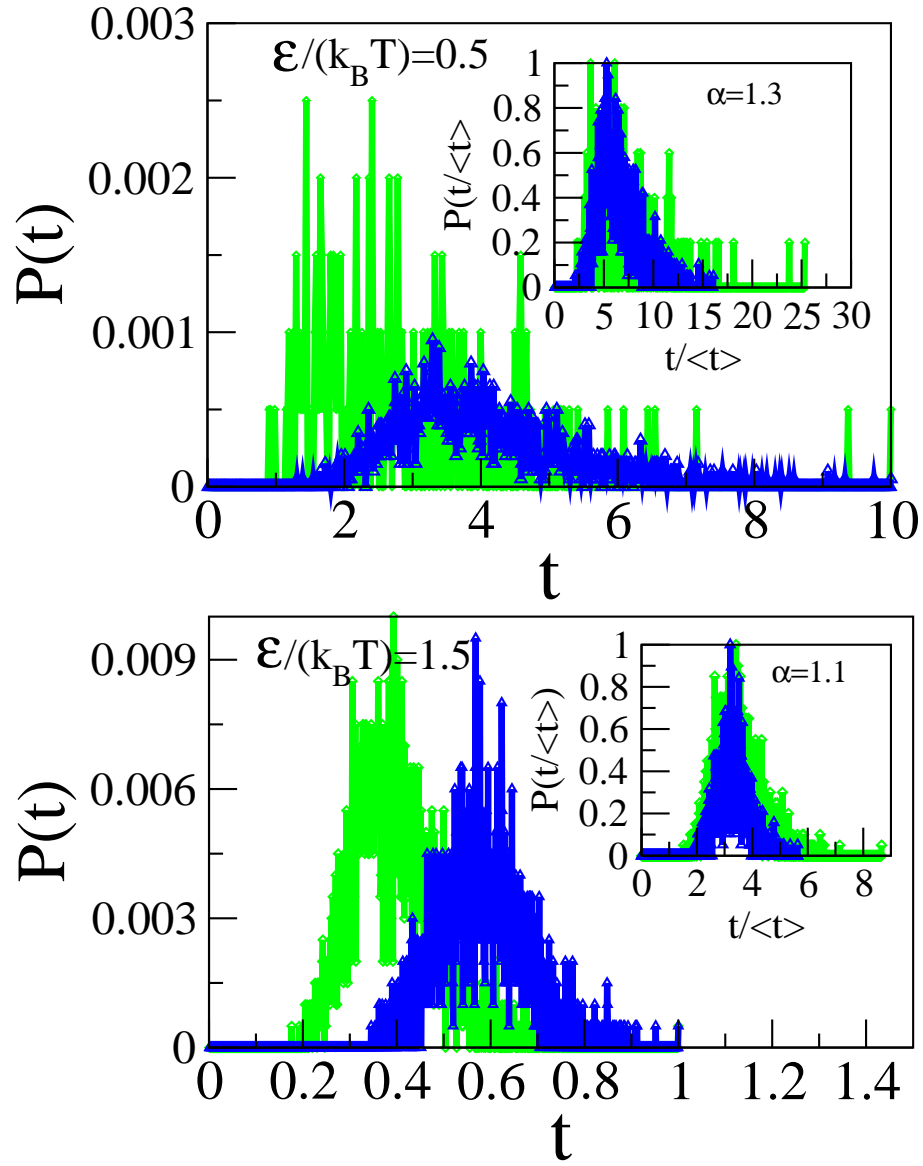


Fig. 10

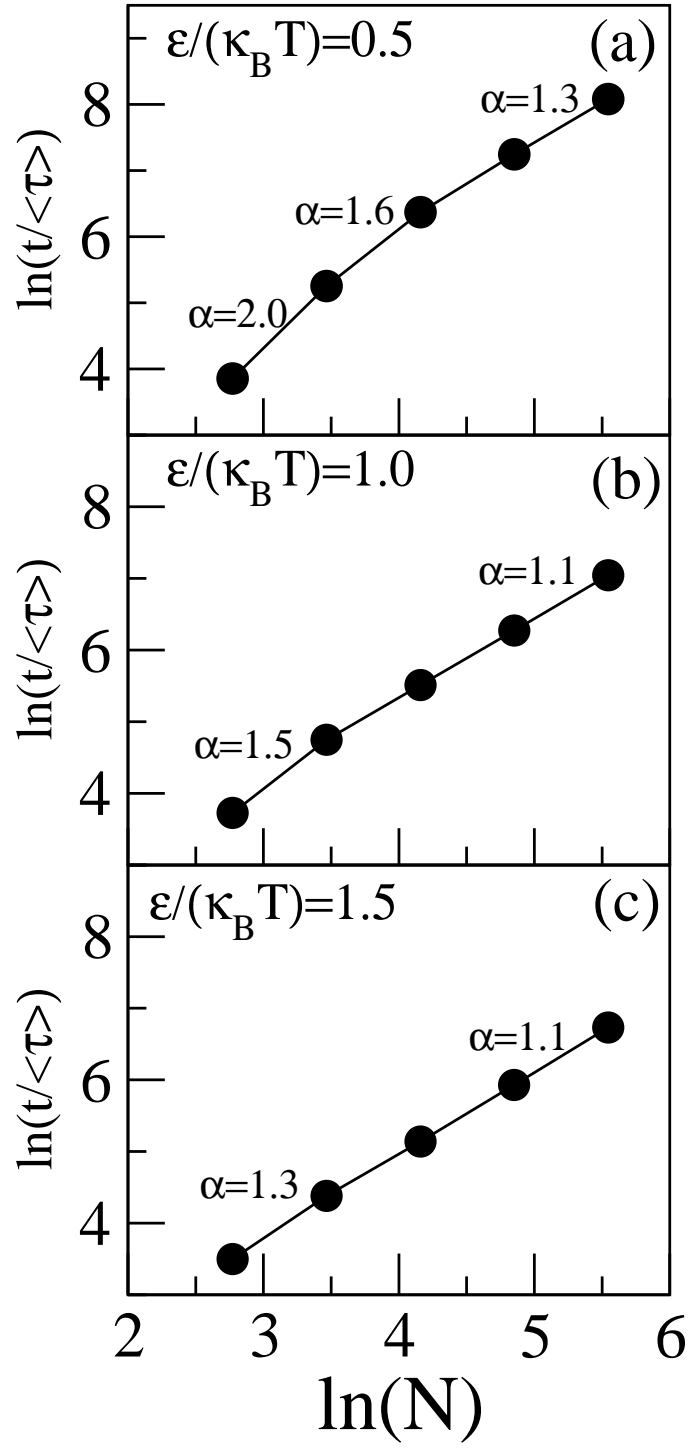


Fig. 11